5th Holistic Innovation in Additive Manufacturing (HI-AM) Conference, Montreal, Canada, 2022.
https://nserc-hi-am.ca/2022/

Real time optimization of bead geometry in robotic wire arc additive manufacturing integrated with supervised learning

Yeon Kyu Kwak[1,2], Thomas Lehmann[1], Mahdi Tavakoli[2], Ahmed Qureshi[1]

1- Additive Design and Manufacturing Systems (ADaMS) Lab, Department of Mechanical Engineering, University of Alberta, Email Address: ykwak@ualberta.ca; lehmann@ualberta.ca; ajqureshi@ualberta.ca
2- Telerobotic and Biorobotic Systems (TBS) group, Electrical and Computer Engineering, University of Alberta, Edmonton, Alberta, T6G 2R3, Canada
Email Address: mahdi.tavakoli@ualberta.ca

Abstract: *Wire Arc Additive Manufacturing (WAAM) is a manufacturing technology that can fabricate a large-scale metallic part in a layer-by-layer fashion. It is receiving great attention from industries as a viable method of manufacturing due to its high deposition rate and cost-efficiency. However, there still exist numerous challenges that need to be overcome to ensure the geometrical accuracy of the part produced. WAAM process is highly non-linear and multi-dimensional and is difficult to model the input process parameters to the output geometrical quality of the final part, especially with an increasing number of materials introduced to WAAM. To overcome this challenge, a supervised learning control algorithm is implemented to search for a parameterized welding process while optimizing the geometry of a single-track multi-layer bead. The input parameters include torch travel speed, wire feed speed, previous layer's geometrical data, and dwell time. The output parameter is the geometry of the printed bead. The proposed algorithm is implemented and validated on a 3-axis gantry WAAM system.*

Keywords: *Additive manufacturing, Process control, Supervised learning*

1 Introduction

Wire arc additive Wire arc additive manufacturing (WAAM) has been receiving great attentions from industries and academia due to its numerous advantages over traditional subtractive manufacturing [1]. It is capable of fabricating large-scale complex metallic components as well as low buy-to-fly ratio [2]. One of the main challenges that limit the full potential of WAAM is its lack of manufacturing accuracy. As WAAM fabricates a component in a layer-by-layer fashion, a buildup of an error may occur where a small error in a previous layer would gradually build up throughout every layer, further negatively affecting the geometrical accuracy of produced part. There exist various input parameters that affect the geometrical accuracy of the final part, and they are often difficult to control as they are highly non-linear and coupled [3]. To overcome this challenge, control of process parameters is required as it would be able to rectify errors and correct itself throughout the manufacturing process. However, WAAM is a very complex time-variant dynamic process with many different process parameters. Some of the input process parameters include torch travel speed and wire feed rate. Observable process parameters that impact the quality of the layered beads include thermal, geometrical information of already deposited beads of the previous layer.

Heralic et al. [4] used a 3D laser scanner to obtain a profile of each layer after every deposition. Through iterative learning control, the deviation of height was adjusted by controlling the wire feed speed for the next deposition layer. Xiong et al. [5] established an improved self-learning neuron feedback control of bead width with a visual sensor and its corresponding image processing algorithm. Doumanidis and Kwak [6, 7] used a laser scanner and infrared sensor to monitor the gas metal arc welding (GMAW) system. A simultaneous but independent closed-loop control of bead width and reinforcement height to the desired specification was achieved. Smith et al. [8] used a CCD camera to capture the image of the molten pool surface and obtained the width of its molten pool. This data was then used on a closed-loop control of a GTAW system as a feedback signal to control weld penetration. Fan et al. [9] implemented feedback control to monitor welding penetration using temperature data. An infrared sensing system monitors the surrounding temperature of the melt pool during a welding process. Liu and Zhang [10, 11] developed a linear-model-based predictive controller to control the 3D weld pool geometry of a GTAW process. Dharmawan et al. [12] proposed a reinforcement learning control framework for controlling layer height. The wire feed rate and torch travel speed were dynamically adjusted according to the measured height using a laser 3D scanner.

Despite the effort of modeling and controlling the WAAM process, in the above reviewed literature, there are other relevant parameters that were not considered. For instance, one would optimize bead height but not width. Often one of the process parameters such as the torch travel speed is held constant in a feedback control loop. This called for a use of control algorithms and techniques that considers many more of the process parameters.

This paper proposes a method of sensor-based in-situ control of robotic WAAM integrated with reinforcement learning (RL) and supervised learning (SL) techniques. The algorithm used is called reinforced inverse supervised learning. The control algorithm is applied to the WAAM system to iteratively collect data from experiment in real time to reinforce the supervised learning neural networks to model the input and output relations to ultimately achieve desired geometrical quality of a single-track multi-layered wall. After sufficient training data and model is developed, the system can identify the best possible action parameters to be chosen given the state of the environment. The action parameters include wire feed speed and torch travel speed. The observable state includes previously deposited layer's geometrical and thermal data. The major advantage of the method is that it can adjust the wire feed rate and the travel speed in accordance with real-time sensory information from a profilometer and an infrared camera to achieve specified geometrical quality. The experiment is conducted to show its effectiveness towards achieving a geometrical conformance of single-track multi-layer wall

2 Supervised learning

Supervised learning is applied when the training data is given in form of input and output target value pairs [13]. Supervised learning algorithm learns the mapping function that models the input to output relation. It is utilized when specific goals are identified to be accomplished from specific set of inputs. It is a "task-driven approach" [14].

Supervised learning can be classified into a classification or a regression problem. First, classification algorithms are used in supervised learning to address problems in which the output variable is categorical, such as male or female, good or bad and yes or no. The classification algorithm can predict the outcome based on the input. Popular example of application of classification is spam filtering. Next, regression is used to solve problems that has a correlation between the input and output variables. Regression finds this correlation to predict continuous output variables given input variables. Weather prediction is one example of supervised learning regression problem.

3 Experimental setup

3.1 Profile sensor

The profilometer utilized in the experiment is SICK PRO2-N100B25A1. It is capable of high-precision measurements by emitting a band-shaped laser beam and using a light-plane-intersecting method that triangulates the reflected light. The reflected light from the emitted band-shaped laser beam is received by the CMOS (complementary metal oxide semiconductor) light receiving unit and the profile is obtained using the resulting image data. The schematic diagram of the profiler measurement can be seen in the Figure 1. It has a measuring distance that ranges from 75 mm to 125 mm away from the light emitting unit, and measuring width ranging from 17 mm to 27 mm. It uses RS-485 serial communication with laser class of 2.

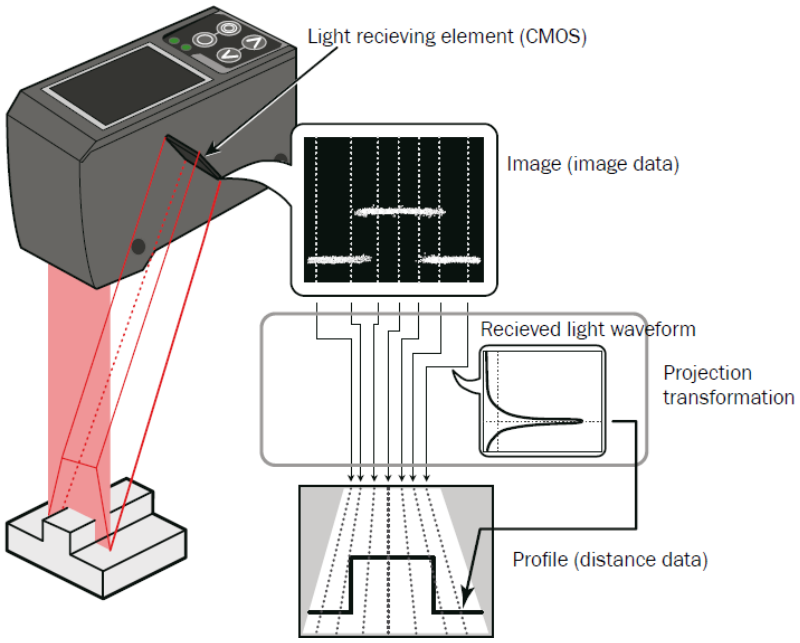

Figure 1 Schematic diagram of SICK profilometer measurements [15]

Profiler was mounted on an instrumentation rig that was attached to the neck of the torch. This setup enabled in-situ monitoring of each layer of bead deposited.

3.2 Thermal sensor

Short wavelength IR (infrared) camera, Optris PI 1M is used to measure the temperature of the printing part in real-time for dwell time control. It is suitable for temperature measurements in metal as this IR camera exhibit distinctly higher emissivity at the short measurement wavelength of 1μm than at the measurements in the conventional wavelength range of 8 ~ 14 μm. It has fast reaction time of 1ms with high dynamic CMOS detector with 764 x 480 pixel resolution with temperature measurement ranging from 450 to 1800 °C. The accuracy of the IR camera is ± 5.0 °C at the room temperature and is ±1% for temperature under 1400 °C.

An IR camera was setup on a tripod aloof of the location of deposition such that the field of view of the camera captures the entirety of the build process from the first to the last layer. The highest temperature of the bead under the perspective of camera is obtained then transmitted to the main controller at frequency of 10 Hz. When the controller is received with the highest temperature data that is below a specified threshold, the dwell time is signaled to end to resume the deposition process of the following layer.

Figure 2 Optris PI 1M infrared camera with CMOS detector

3.3 Software hardware interface

The experiment was conducted with multitude of devices connected to one another. The overview of the system process is shown in Figure 3 Software and hardware interface and system flow diagram.

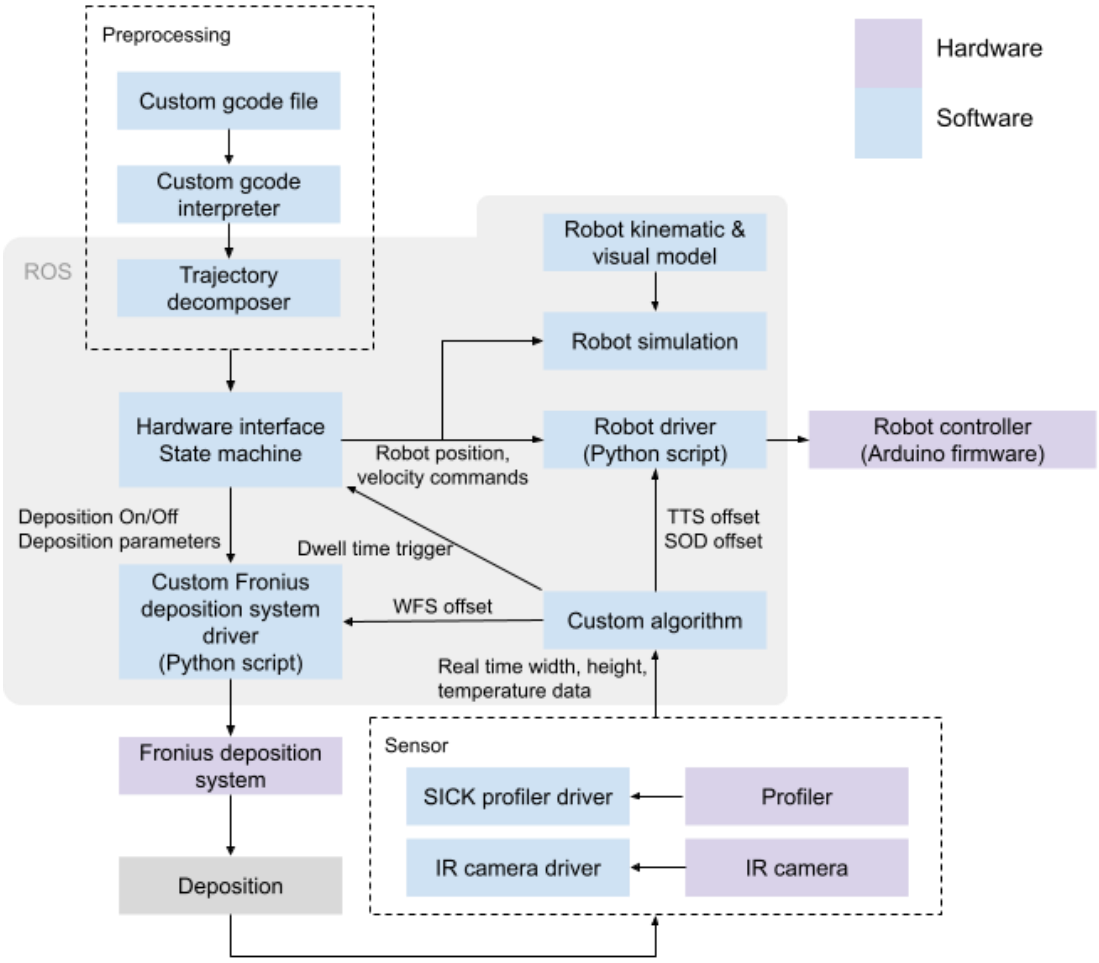

Figure 3 Software and hardware interface and system flow diagram

Starting with pre-processing stage where the custom gcode file is in input to the ROS head controller, the deposition takes place while the sensors are actively measuring the system output. This real-time data from the sensors such as geometry data from profiler and thermal data of the IR camera are fed back into the custom algorithm where it can command the deposition parameters to change. The welding wire used for the study is ER70S.

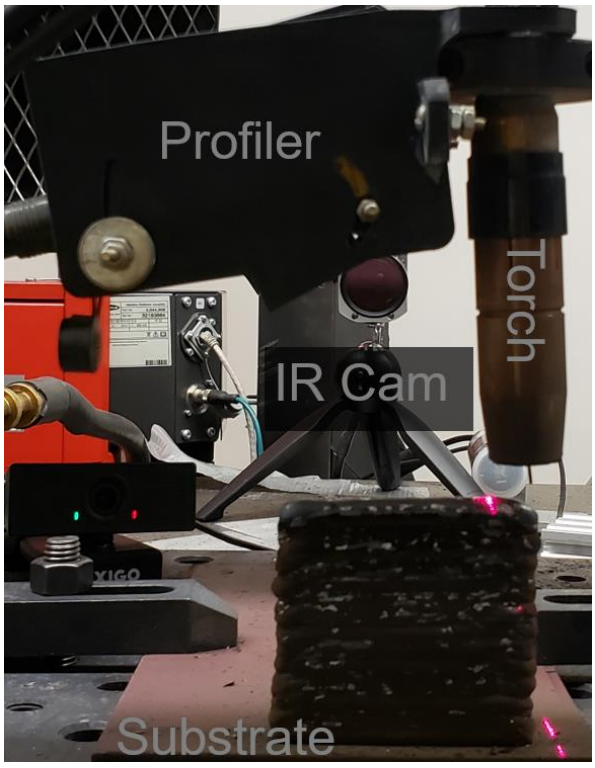

Figure 4 Close view of setup at location of deposition

4 Methodology

4.1 Reinforced supervised learning inverse control

To find the optimal wire feed speed and torch travel speed to output desired layer width and height, a supervised learning inverse control algorithm framework is applied. This framework utilizes historical deposition rollout data model the input to output relation and finally can predict the optimal wire feed speed given desired layer width and height. Also, the framework enhances in robustness during deposition process. With more rollout data, the weights of the neural network are adjusted accordingly in-situ.

4.2 Neural network setup

The thermal, geometrical data of the previously deposited layer, wire feed speed and torch travel speed are set of data composing the input layer of the supervised learning neural network and the output are the deposited layer width and the height. The neural network model that maps the input to the output parameters was initially trained with data from 700 layers of bead deposition or a multiple of 14 different 50 layers walls. During the training stage, the layers were deposited with random wire feed speed for every layer, ranging from 60 inches per minute (IPM) to 120 IPM with interval of 10 IPM.

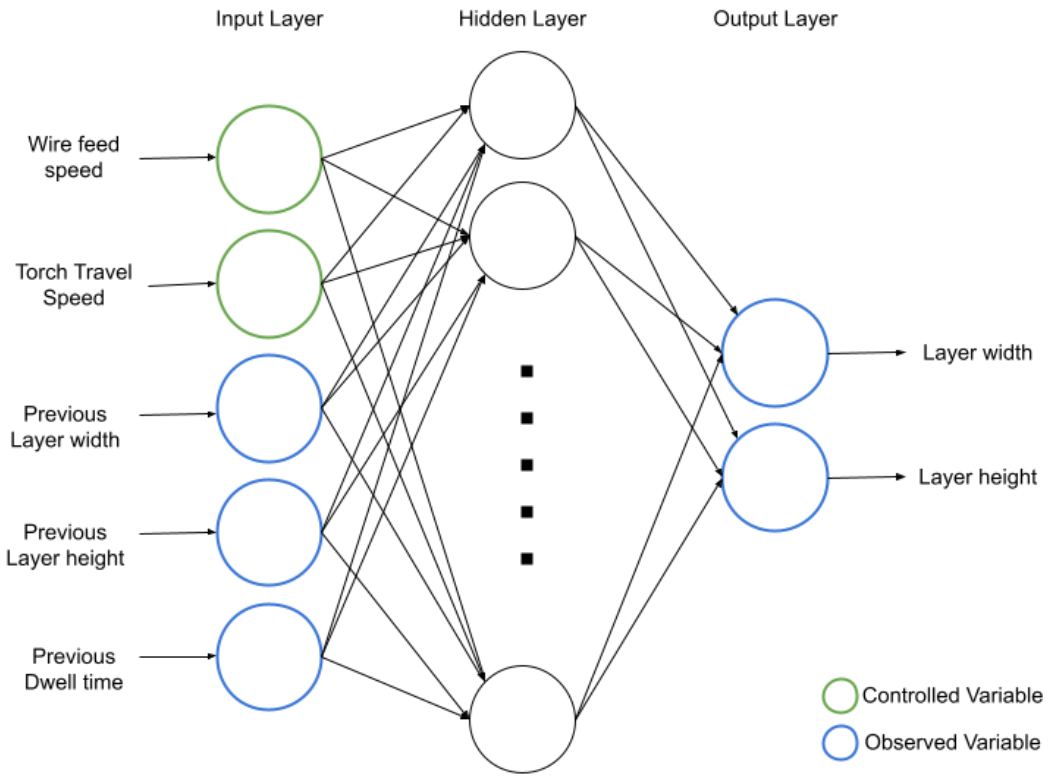

Figure 5 Neural network setup consisting of three layers. Wire feed speed and torch travel speed are set as controlled variables

4.3 First deposited layers initialization

For both training and rollout stage of the experiment, the first layer must be initialized. Deposition of the first layer occurs on the substrate plate with no dwell time and geometrical information of the previously deposited bead. Although the minimum number of layers that must be deposited prior to deploying the control algorithm is one, the initialization is done with deposition of two layers. This is because the first layer is a special case where the deposition occurs on a cool surface, causing the bead to be very different in size in relation to the following layers. Subsequently, the second layer is also considered a special case as the deposition occurs on top of the first layer. Thus, the first two layers are deposited with a fixed input process parameter. The wire feed speed is set as 90 IPM and 350 cm/min as the torch travel speed for the first two layers initialization. After the initialization layers have been deposited, the dwell time, layer width and height of the consequent layers are monitored and measured.

4.4 Control algorithm

The control algorithm given layer width, height and the dwell time of the previous layer can predict the optimal wire feed speed where the optimality criteria is set by a reward function. The policy in choosing the optimal wire feed speed is as follows:

$$\pi = \underset{WFS_i, TTS_j}{\text{argmax}} \, (reward)$$

Where,

$$reward = -|Desired\ width\ - layer\ width| - \frac{|Desired\ height - layer\ height|}{importance\ weight}$$

The various level of the wire speed available is denoted as i. The wire speed level ranges from 60 to 120 IPM, inclusive with interval of 5 IPM. Although the training of the neural network was trained with a broader interval of 10 IPM, the wire feed speed was interpolated to maximize the reward function. The importance weight represents the magnitude at which it diminishes the importance

of the height error. An exemplary graph showing how the algorithm decides on the optimal wire feed speed based on the reward calculated with the neural network modeled function is illustrated in Figure 6 Schematic of how reward is perceived by the model created by the supervised learning neural network. Dwell time is also in place as an extra controller to wait for the system to cool down to 600 °C.

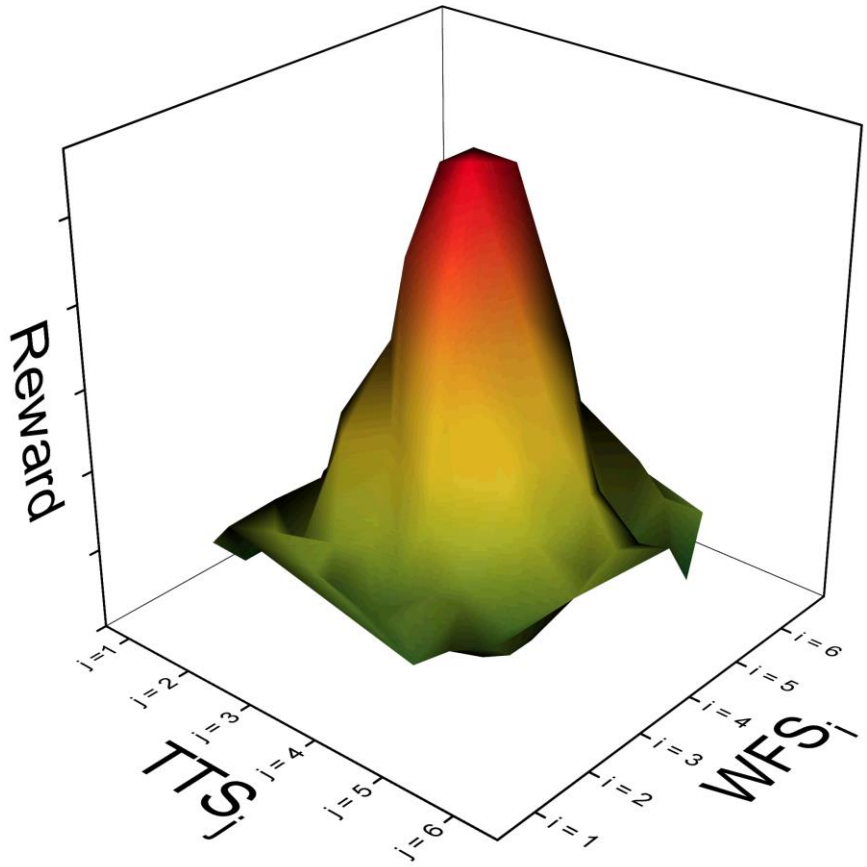

Figure 6 Schematic of how reward is perceived by the model created by the supervised learning neural network

Algorithm 1. Inverse supervise learning method

Initialize neural network layers with random weights
Pretrain the neural network dynamics function, $\widehat{f_\theta}$ with historical data tuple of $D_n = \{(WFS_1, TTS_1, LW_1, LH_1, DT_1, LH_2, LW_2) \dots (WFS_n, TTS_n, LW_n, LH_n, DT_n, LH_{n+1}, LW_{n+1})\}$ Where n represents number of data tuples
Initialize first layers
Observe LH_1, LW_1, DT_1
For layer number i to max number of layers, **do**:
  Predict LH_{i+1}, LW_{i+1} with dynamics function $\widehat{f_\theta}$
  Perform optimal action, WFS_i, TTS_i
  Observe LH_{i+1}, LW_{i+1}
  Append $D_i = (WFS_i, TTS_i, LW_i, LH_i, DT_i, LW_{i+1}, LW_{i+1})$ to D_n
  Train $\widehat{f_\theta}$ using D
End for

---

5 Results and discussion

With pretraining of neural network dynamic function, $\widehat{f_\theta}$ with 200 pretraining data tuples, new walls are deposited with target width of 5 mm and 5.5 mm. The pretraining was done using random policy.

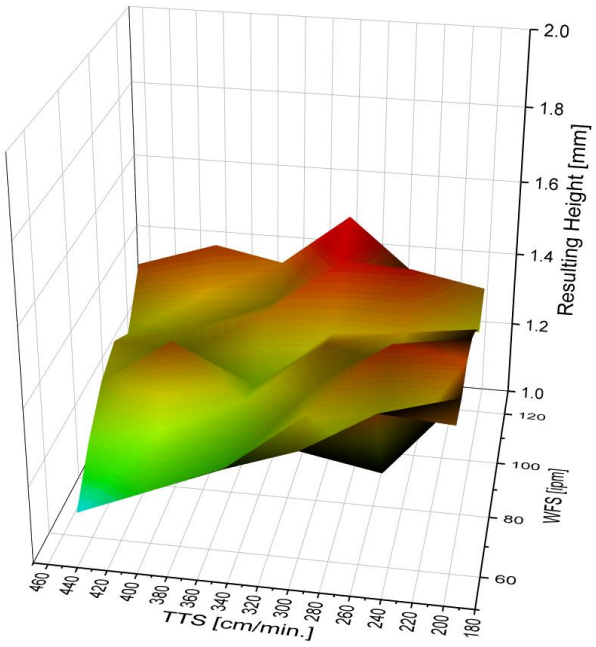

Figure 7 200 random policy datasets visualized with resulting height as function of TTS and WFS

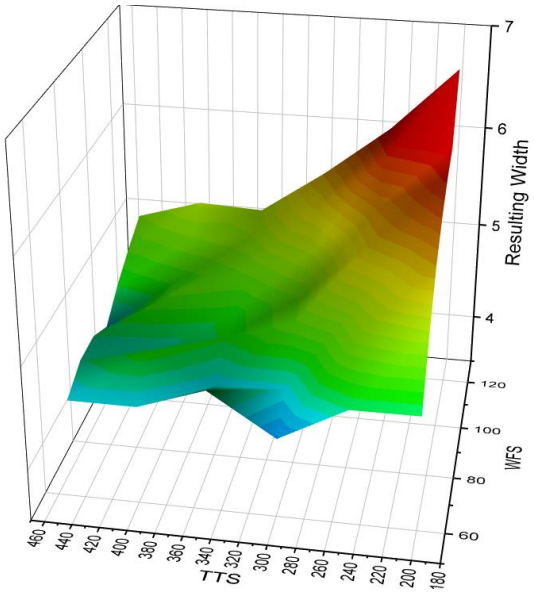

Figure 8 200 random policy datasets visualized with resulting width as function of TTS and WFS

Despite the effects of previous layer's geometry and thermal data is not illustrated in the 3D plots of Figure 7 200 random policy datasets visualized with resulting height as function of TTS and WFS and Figure 8 200 random policy datasets visualized with resulting width as function of TTS and WFS, there is an evident trend in how TTS and WFS are negatively and positively correlated to both of the resulting width and height, respectively. Using the training data, the supervised learning neural network was trained to learn the model of the system. With 200 layers worth of training dataset, 4 walls were printed with two different target width. First two walls were printed to have 5.5 mm as width and latter two as 5 mm. Target height for all experiments were set to 1.3 mm as it is the distance increment for the gcode to deposit every layer. The importance weight was set as 6 for all experiments to have the algorithm prioritize tracking the width more than the height.

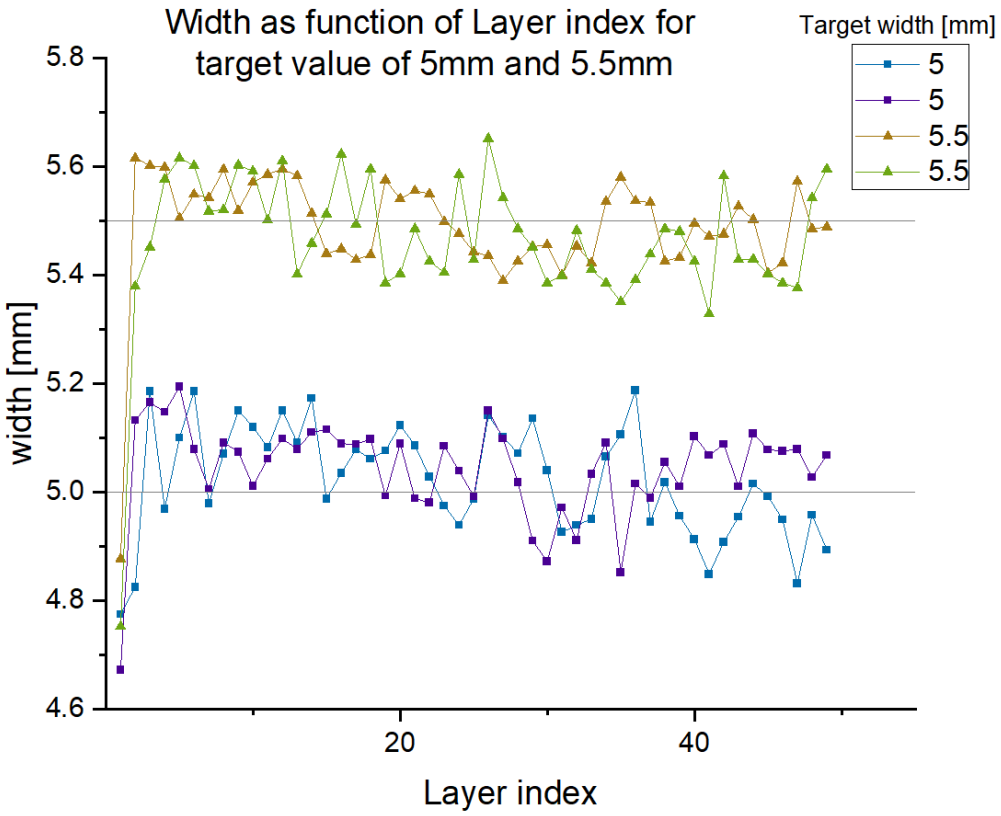

Figure 9 Width of the bead as a function of number of layers deposited

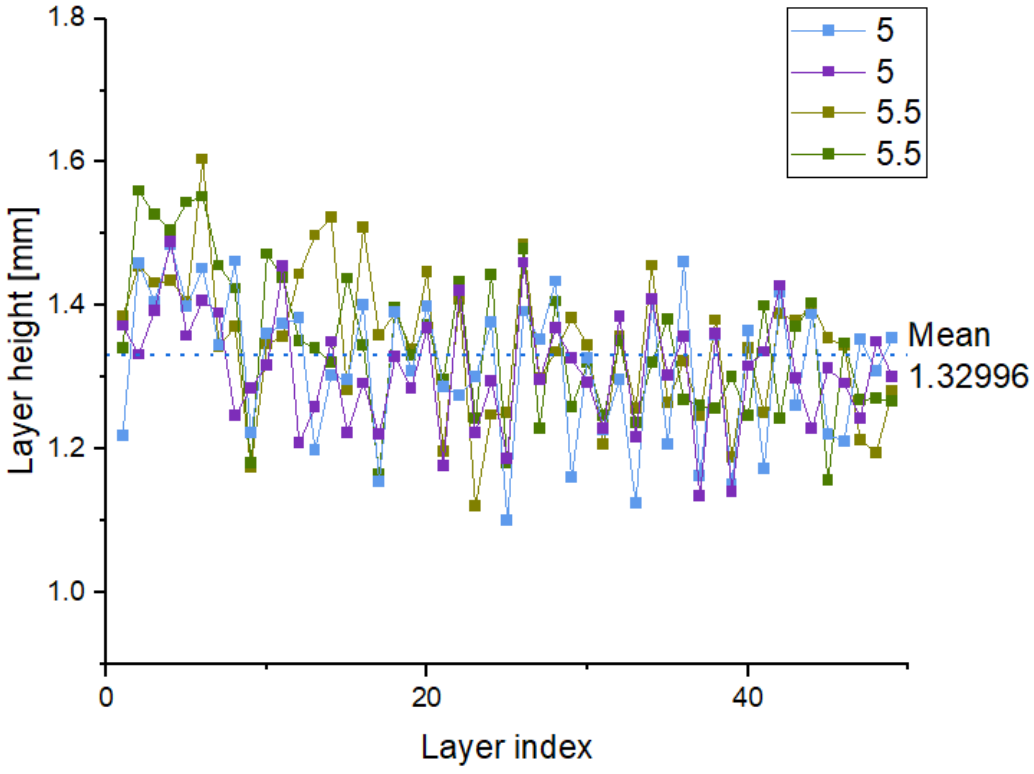

Figure 10 Height of the bead as a function of number of layers deposited, with varying target width

The result show that both the width and height of the wall tracks the specified target value of 5 mm and 5.5 mm for width and 1.3 for the height. Also, the tracking performance enhances as number of deposited layers increase. This may be due to accumulation of more data appended into the training dataset to provide more accurate model and prediction. This relatively low tracking for the first few layers also may have happened due to the generalization of the supervised learning model, generalizing the higher layer deposition process to that of the lower layers. For example, as the training dataset were obtained from producing four sets of 50 layered wall, most of the data constitutes the deposition process at high temperature environments.

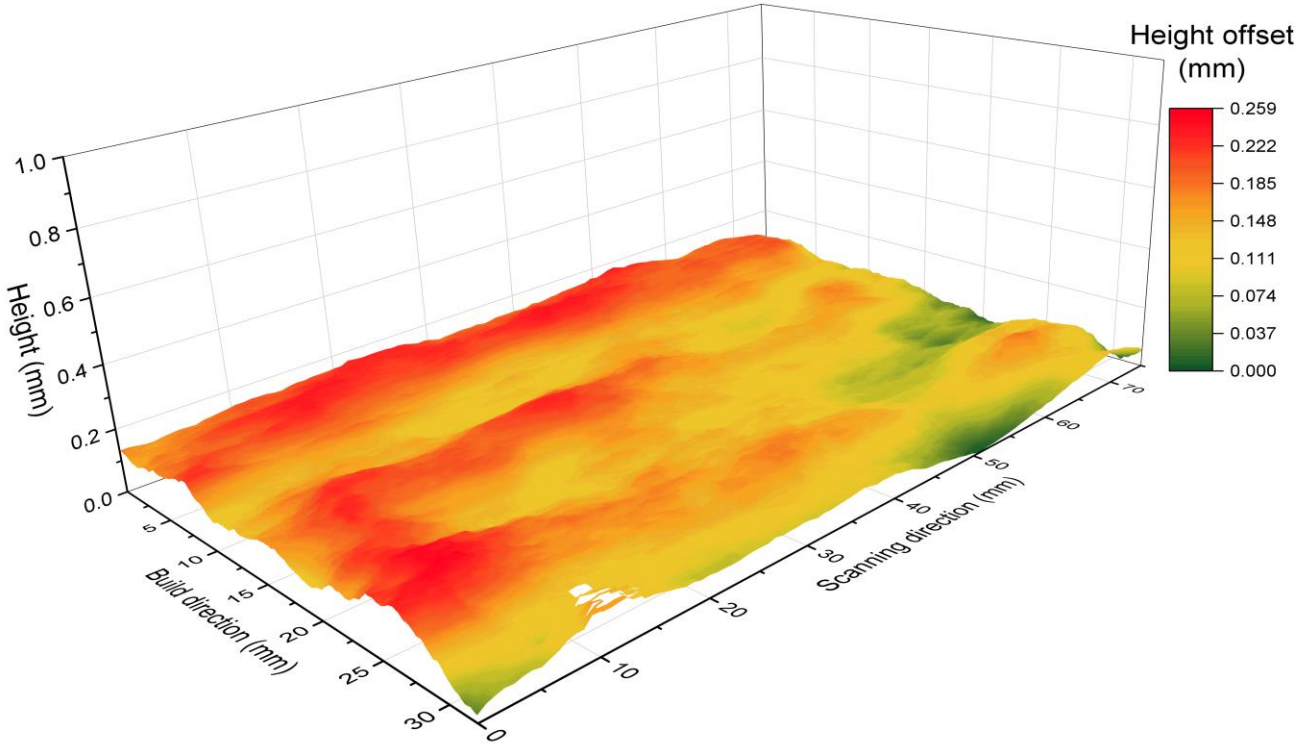

Figure 11 Side profile of the first deposited wall of desired width of 5.5mm

The side profile of the first printed wall with target width of 5.5 mm is shown in Figure 11. The largest dimensional error in terms of width is shown to be 0.259 mm. The scanned area is a partial to the middle of the wall with dimension of 32 mm by 75 mm this equates to approximately 25 layers of deposited part.

6 Conclusion

Through Reinforced supervised learning inverse control, 50 layered walls of varying target geometry were deposited. The algorithm uses previously trained dataset in tuple of previous layer's width, height, wire feed speed, torch travel speed, dwell time and resulting width and height to model the supervised learning neural network. The learned model is then used to predict the best sets of wire feed speed and torch travel speed, given the information of the previously deposited wall's width and height. Through printing walls with target width of 5.5mm and 5mm both with target height of 1.3mm, the algorithm showed great tracking performance for both width and height as layer number increased. The height tracking performance was great as well, giving average height of 1.330 mm, deviating only 0.03 mm from the desired height. The algorithm reinforces itself in-situ every layer by appending the obtained data from the sensors to the training dataset for the neural network. The future studies to be done is first, testing the system for robustness to disturbance and next, to optimize the neural network architecture to make the system more sample efficient and analyze how many samples are required to output satisfactory tracking performance. Then the similar experiments are to be done with higher geometrical complexity such as a part that contains various angles.

Acknowledgment

This research is supported by the NSERC HI-AM Strategic Partnership Grant No. 494158.

References

[1] Xia, C., Pan, Z., Polden, J., Li, H., Xu, Y., Chen, S., & Zhang, Y. (2020). A review on wire arc additive manufacturing: Monitoring, control and a framework of automated system. *Journal of Manufacturing Systems*, *57*, 31-45.

[2] Williams, S. (2015). Wire+ arc additive manufacturing vs. traditional machining from solid: a cost comparison.

[3] Xia, C., Pan, Z., Polden, J., Li, H., Xu, Y., Chen, S., & Zhang, Y. (2020). A review on wire arc additive manufacturing: Monitoring, control and a framework of automated system. *Journal of Manufacturing Systems*, *57*, 31-45.

[4] Heralić, A., Christiansson, A. K., & Lennartson, B. (2012). Height control of laser metal-wire deposition based on iterative learning control and 3D scanning. *Optics and lasers in engineering*, *50*(9), 1230-1241.

[5] Xiong, J., Zhang, G., Qiu, Z., & Li, Y. (2013). Vision-sensing and bead width control of a single-bead multi-layer part: material and energy savings in GMAW-based rapid manufacturing. *Journal of cleaner production*, *41*, 82-88.

[6] Doumanidis, C., & Kwak, Y. M. (2001). Geometry modeling and control by infrared and laser sensing in thermal manufacturing with material deposition. *J. Manuf. Sci. Eng.*, *123*(1), 45-52.

[7] Doumanidis, C., & Kwak, Y. M. (2002). Multivariable adaptive control of the bead profile geometry in gas metal arc welding with thermal scanning. *International Journal of Pressure Vessels and Piping*, *79*(4), 251-262.

[8] Pires, J. N., Smith, J. S., & Balfour, C. (2005). Real-time top-face vision based control of weld pool size. *Industrial Robot: An International Journal*.

[9] Fan, H., Ravala, N. K., Wikle III, H. C., & Chin, B. A. (2003). Low-cost infrared sensing system for monitoring the welding process in the presence of plate inclination angle. *Journal of materials processing technology*, *140*(1-3), 668-675.

[10] Liu, Y. K., & Zhang, Y. M. (2013). Model-based predictive control of weld penetration in gas tungsten arc welding. *IEEE Transactions on Control Systems Technology*, *22*(3), 955-966.

[11] Liu, Y., & Zhang, Y. (2013). Control of 3D weld pool surface. *Control Engineering Practice*, *21*(11), 1469-1480.

[12] Dharmawan, A. G., Xiong, Y., Foong, S., & Soh, G. S. (2020, May). A Model-Based Reinforcement Learning and Correction Framework for Process Control of Robotic Wire Arc Additive Manufacturing. In 2020 IEEE International Conference on Robotics and Automation (ICRA) (pp. 4030-4036). IEEE.

[13] J. Han, M. Kamber, and J. Pei, Data Mining: Concepts and Techniques. 2012. doi: 10.1016/C2009-0-61819-5.

[14] I. H. Sarker, A. S. M. Kayes, S. Badsha, H. Alqahtani, P. Watters, and A. Ng, "Cybersecurity data science: an overview from machine learning perspective," Journal of Big Data, vol. 7, no. 1, 2020, doi: 10.1186/s40537-020-00318-5.

[15] SICK Ltd, Profiler 2 Short range distance sensor operating instructions. 2019